Hindawi Publishing Corporation
Advances in Meteorology
Volume 2016, Article ID 8582041, 10 pages
http://dx.doi.org/10.1155/2016/8582041

Research Article

Impact of DEM Resolution and Spatial Scale: Analysis of Influence Factors and Parameters on Physically Based Distributed Model

Hanchen Zhang,[1,2] Zhijia Li,[1,2] Muhammad Saifullah,[1,2] Qiaoling Li,[1,2] and Xiao Li[3]

[1]*College of Hydrology and Water Resources, Hohai University, Nanjing 210098, China*
[2]*National Cooperative Innovation Center for Water Safety & Hydro-Science, Hohai University, Nanjing 210098, China*
[3]*North China University of Water Resources and Electric Power, School of Water Conservancy, Zhengzhou 450045, China*

Correspondence should be addressed to Hanchen Zhang; zhang_hanchen520@163.com

Received 10 May 2016; Revised 11 August 2016; Accepted 14 September 2016

Academic Editor: Francesco Viola

Physically based distributed hydrological models were used to describe small-scale hydrological information in detail. However, the sensitivity of the model to spatially varied parameters and inputs limits the accuracy for application. In this paper, relevant influence factors and sensitive parameters were analyzed to solve this problem. First, a set of digital elevation model (DEM) resolutions and channel thresholds were generated to extract the hydrological influence factors. Second, a numerical relationship between sensitive parameters and influence factors was established to define parameters reasonably. Next, the topographic index (TI) was computed to study the similarity. At last, simulation results were analyzed in two different ways: (1) to observe the change regularity of influence factors and sensitive parameters through the variation of DEM resolutions and channel thresholds and (2) to compare the simulation accuracy of the nested catchment, particularly in the subcatchments and interior grids. Increasing the grid size from 250 m to 1000 m, the TI increased from 9.08 to 11.16 and the Nash-Sutcliffe efficiency (NSE) decreased from 0.77 to 0.75. Utilizing the parameters calculated by the established relationship, the simulation results show the same NSE in the outlet and a better NSE in the simple subcatchment than the calculated interior grids.

1. Introduction

Digital Elevation Model (DEM) data contains abundant topography, geomorphology, and hydrology information, which accelerated the development of physically based distributed hydrological model. As mature software such as ArcGIS and WMS has been completed to extract the information regarding slope, flow direction, and concentration, the spatial relationship between dynamic mechanics of water cycle and surrounding units could be taken into account. Based on conservation of mass, momentum, and energy, as well as catchment runoff and concentration characteristics, these components were deduced by numerical analysis method which makes the physically based distributed hydrological model deemed as a kind of model of high precision, scientificity, and effectivity [1, 2].

Based on the assumption of some hydrological conditions, hydrological model is established on a certain spatial and temporal scale. It is significant to derive and demonstrate the hydrological variables and change factors on different scales [3–7]. Higher DEM resolution provides a more accurate representation of topographic features [8], which makes the data on the small scale more precise and representative. However, the representativeness of small-scale data is doubted when used in large scale [9]. When larger-scale data are converted to small-scale data, there are some critical problems to be considered, such as the heterogeneity and the nonlinear response [10]. Therefore, a complete system of theory and methodology should be constructed [11]. Researchers focused on the scales problem fell largely into two different perspectives. The first perspective, which is proposed by Beven [12], is that two different hydrological models are still needed to solve the problem. One is used to describe the hydrological processes on a small catchment scale in detail while the other one is used to make a hydrological forecast on a larger catchment scale. Beven

believes that only one hydrological model could not solve the scales problem and the scale dependence of distributed hydrological model must be introduced [13]. The second perspective, which is proposed by Blöschl [14], indicates that there is a gradual process of solving the scales problem and eventually there will be significant achievements in theoretic and practical hydrology. The controlling equations of the model are established based on a point scale, which is deemed effective for different catchment scales, without taking into consideration how the model parameters are related to various scales. In practice, current techniques on hydrological measurement have limited the accuracy of observed parameters, and the accuracy of the measured values is much lower than the required unit scale of the model.

The recently developed distributed hydrological models are all physically based and DEM-based, with distributed parameters, input information, process description and results outputs, and hydraulic calculation method [15], which leads to a complex process to calibrate parameters and requires a long time to calculate the flow. The simulation results are strongly influenced by diverse factors, such as topographic characteristics, surface delineation methods, and DEM interpolation/aggregation methods. Generally, lower DEM resolution (or larger grid size) is generated from original higher DEM resolution by using certain interpolation/aggregation methods [16]. However, DEM processing could change the accuracy of input information [17, 18], and parameter calibration could give rise to serious equifinality with different parameters, which leads to an unreliable simulation in interior grids. However, in order to use the model in the study area, DEM processing, parameter calibration, and validation [19] are highly recommended and extremely necessary.

This research was focused on sensitivity analysis [20, 21] of influence factors and parameters, and a numerical relationship between influence factors and sensitive parameters has been established. The selected relationship was used to improve parameter calibration efficiency, avoid overparameterization, and generate more accurate model outputs [22–24]. The aim of the study is to enlarge the applicable scope for physically based distributed hydrological model, improve the simulation accuracy for interior grids, decrease the error caused by low DEM resolution, and provide a basis for parameter transformation. The research has several major objectives as follows. First, we hope to analyze the variations of hydrological information depending on different DEM resolutions, channel thresholds, and catchment scales. Second, we want to develop a numerical relationship between influence factors and sensitive parameters when the influence factors of runoff and concentration parameters are considered comprehensively. Thirdly, we want to make sure that the simulation results with different DEM resolutions and channel thresholds can achieve the same accuracy when the parameters are given by the established relationship. The ultimate objective of this research is to apply the calibrated parameters to improve simulation accuracy in interior grids.

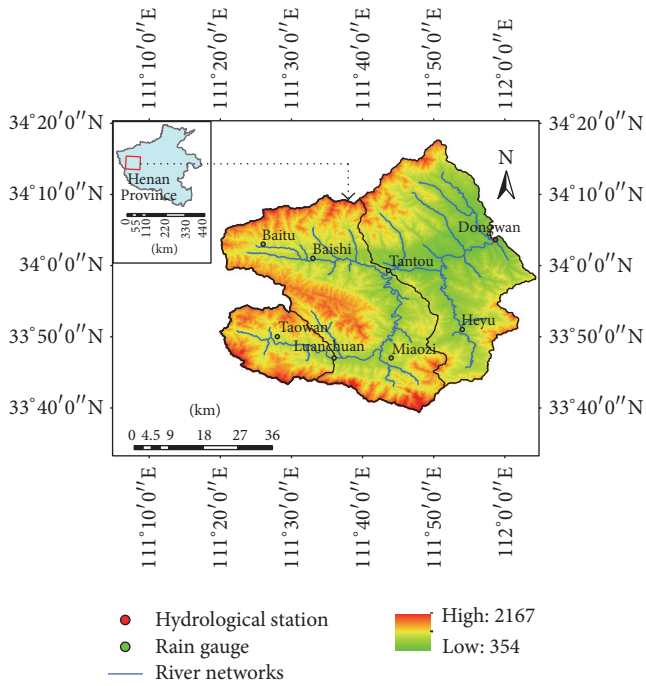

Figure 1: Location, topography, and drainage networks of Dongwan catchment.

2. Materials and Methods

2.1. Study Area. For this research, the study area is located in Yi River Source region which is a tributary of the Yellow River in Henan Province in China. The nested catchment is characterized as a typical semihumid and semiarid area which comprises Dongwan (2569 km^2), Tantou (1839 km^2), and Luanchuan (340 km^2) (Figure 1). In this nested catchment, annual and interannual precipitations are not evenly distributed. Maximum annual precipitation is 2.43–3 times more than the minimum annual precipitation, and precipitation from July to September accounts for more than half of the entire year's precipitation. In general, flood in this catchment is caused by a rainstorm, and has the characteristics of sudden rise and drop, high flood peak, and short duration.

2.2. Data Acquisition. Through DEM and ArcGIS processing, the Luanchuan catchment was processed to 3 kinds of resolutions of 250 m, 500 m, 1000 m, and channel thresholds of 60 for 250 m DEM, 15 for 500 m DEM, and 7.5 and 35 for 1000 m DEM; the Dongwan and Tantou catchment was processed to the resolution of 1000 m and channel thresholds of 35 (Figure 2). Eight precipitation stations are located in Dongwan catchment, 6 in Tantou catchment, and 2 in Luanchuan catchment. Soil types and vegetation types of this study area are relatively simple, so they are just neglected and regarded as a homogeneous underlying surface. The catchment delineation processing was designed to research the changed factors caused by ArcGIS processing and to analyze the sensitive factors (Table 1).

Table 1: Information and statistics of the nested catchments.

Name	DEM resolution	Channel threshold	Area (km^2) (ArcGIS)	Total grids	Water systems numbers
Luanchuan	250	60	347.25	5556	53
	500	15	342.75	1371	44
	1000	35	341	341	6
	1000	7.5	341	341	27
Tantou	1000	35	1839	1839	31
Dongwan	1000	35	2569	2569	40

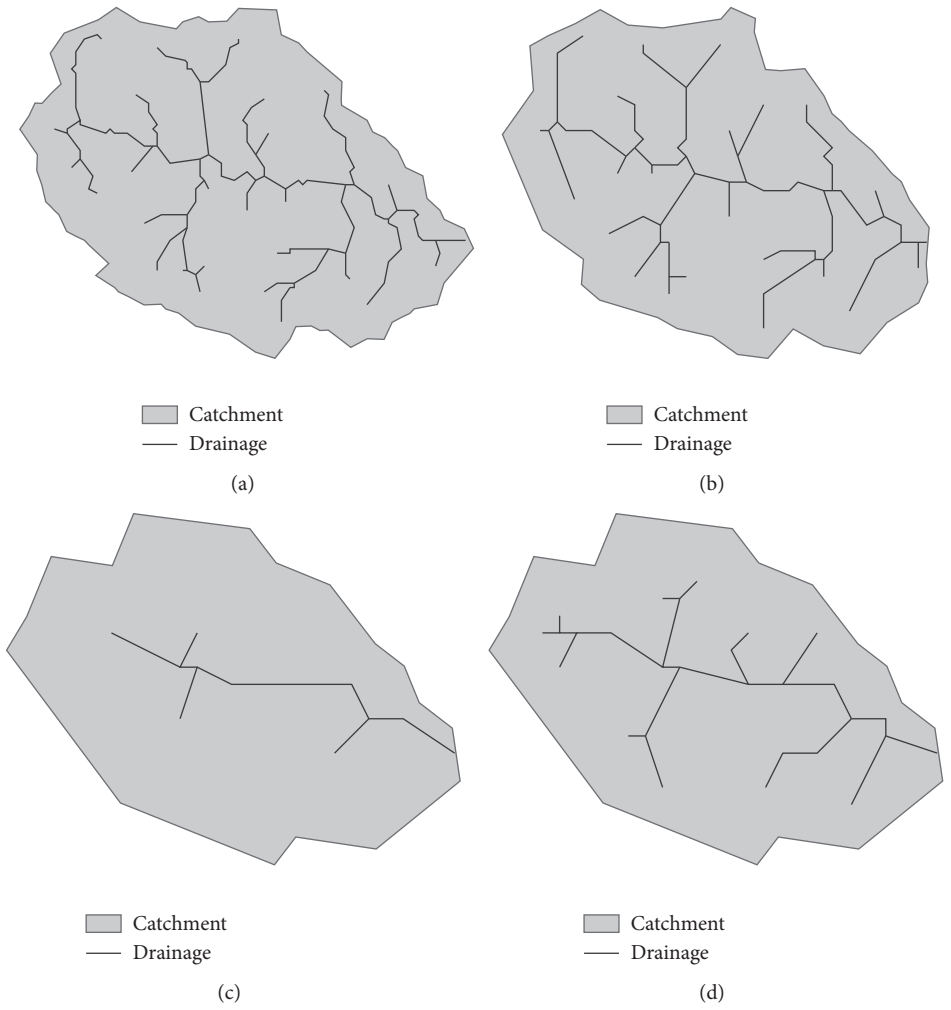

Figure 2: The catchment and drainage networks of Luanchuan, (a) resolution of 250 m, channel threshold of 60, (b) resolution of 500 m, channel threshold of 15, (c) resolution of 1000 m, channel threshold of 35, and (d) resolution of 1000 m, channel threshold of 7.5.

2.3. Overview of CASC2D Model. The CASCade 2 Dimensional (CASC2D) originally begins with a two-dimensional overland flow routing algorithm which was developed and written in APL by Professor Julien at Colorado State University [25–27]. CASC2D has been developed to determine the runoff hydrograph generated from any temporally spatially varied rainfall event. For a given rainfall event, CASC2D model ignores the evapotranspiration during the rain and relies on inverse square distance weighting method for each grid to describe a fully spatially varied rainfall input [28], and once the initial soil moisture deficit has been supplied by rainfall, water begins to infiltrate. This step requires the adoption of an infiltration scheme that can predict the portion of the rainfall that drains into the ground. The Green & Ampt [29, 30] infiltration equations accommodate spatial and temporal variabilities due to changes in rainfall and soils properties and take into account the accumulated infiltration. Using a Hortonian overland flow process, when the precipitation rate exceeds the infiltration rate, the excess rainfall will accumulate as surface water and begin to flow.

Table 2: Statistics information of influence factors.

Name	Resolution and threshold	Station number (controlled area/km^2)	Slope/°	Total grids in stream links (area channel ratio)	L_0/km	$S_{f_0}/\tan\alpha$	L_1/km	$S_{f_1}/\tan\alpha$
Luanchuan	250_{60}	2 (170)	12.09	429 (0.81)	428.64	0.185	39.78	0.0140
	500_{15}		8.56	199 (1.72)	422.87	0.167	36.46	0.0149
	$1000_{7.5}$		6.33	65 (5.25)	634.82	0.124	29.64	0.0145
	1000_{35}		6.33	28 (12.2)	1289.79	0.153	27.75	0.0141
Tantou	1000_{35}	6 (307)	5.98	179 (10.3)	7515.33	0.215	76.25	0.0155
Dongwan	1000_{35}	8 (321)	5.67	257 (10.0)	11010.55	0.245	109.31	0.0158

Overland flow is routed into the channels using a 2D diffusive wave equation ((1)–(4)). In channels, the water is routed using a 1D diffusive wave equation [31] ((5)-(6)).

$$S_{f_0} = S_0 - \frac{\partial h}{\partial (x, y)}, \tag{1}$$

where, S_{f_0} is friction-resistance gradient of slope concentration in the x- and y-direction, respectively; S_0 is the gradient of slope concentration in the x- and y-direction, respectively; $\partial h/\partial(x, y)$ is an additional gradient of slope concentration in the x- and y-direction, respectively.

$$q = \alpha h^{\beta}, \tag{2}$$

where q is the discharge per unit width; h represents the depth of surface runoff; α and β depend on the flow state and the turbulent flow.

$$\alpha = \frac{1}{n_0} \left(S_{f_0}\right)^{1/2} \frac{S_{f_0}}{\left|S_{f_0}\right|}$$
$$\beta = \frac{5}{3}, \tag{3}$$

where $S_{f_0}/|S_{f_0}|$ determines the flow direction and n_0 represents the Manning roughness coefficient of slope concentration.

$$Q = \frac{1}{n_1} A R^{2/3} S_{f_1}^{1/2}, \tag{4}$$

where n_1 is the Manning roughness coefficient of the channel, R is the hydraulic radius, S_{f_1} is the friction-resistance gradient of the channel, and A is the cross-sectional area.

$$S_{f_1} = S_1 - \frac{\Delta h}{\Delta x}, \tag{5}$$

where S_1 is the gradient of the channel and $\Delta h/\Delta x$ is an additional gradient.

CASC2D is built on finite difference and finite volume numerical schemes and thus operates upon a uniform grid. This gridded approach allows spatial variability in watershed characteristics to be distributed across an entire basin at user-selected grid sizes [32]. Small grid sizes are used when the physically based parameters can be accurately observed and spatially interpolated. However, larger grid sizes may be preferred because the spatial variability of catchment characteristics is not explicit and computational efficiency is an important issue [33]. Actually, it is unrealistic to use small grid sizes in very large catchment or large numbers of events. Within a given catchment, input information (e.g., catchment area, stream links, soil distribution, and vegetation distribution) is defined through ArcGIS processing of DEM data. These geometric characteristics are used as the hydrological model components of CASC2D.

2.4. Statistics of Influence Factors. The input data processing would cause some uncertainty in the process of DEM resolution conversion and drainage extraction by ArcGIS. On a statistical-information basis, some hydrological factors were calculated to analyze the sensitivity. CASC2D model divides the concentration process into two sections; one is slope concentration, and another is channel concentration. So the traditional concentration factors should be considered more specifically. This section describes the change of statistic and calculated hydrological factors after DEM and ArcGIS processing. The related hydrological factors are (1) the precipitation station number in the study area and the controlled area for every station; (2) total grids in stream and the ratio of catchment area and total grids in stream; (3) average slope for the study catchment in different DEM resolutions; (4) the slope concentration route distance L_0 and the average concentration slope S_{f_0} for every DEM resolution and channel threshold calculated by D8 (deterministic eight neighbors) algorithm; and (5) the permanent main channel length L_1 and the permanent main channel gradient S_{f_1} for every DEM resolution and channel threshold. Based on the original data and processed data, the major influence factors for nested catchment under different DEM resolutions and channel thresholds are calculated and summarized (Table 2).

2.5. Sensitive Factors of the Model. CASC2D model is a physically based model with physical-equations-controlled runoff process and concentration process. The calibrated parameters are analyzed to improve relationships between model parameters and hydrological characteristics (i.e., precipitation, area, soils, vegetation, and topographic features). Researchers have found out that the average slope of the catchment is reduced along with the decrease of resolution [34–37]. However, the average slope of catchments could not fully represent the concentration process. So the average concentration slope and concentration route distance were

Table 3: Relations among concentration parameters.

Relation		Slope concentration			Channel concentration		
		$S_{f_0}^{1/2}$	L_0/km (unit area)	n_0	$S_{f_1}^{1/2}$	L_1/km (unit area)	n_1
Luanchuan	500 : 250	0.950	0.986	0.963	1.032	0.917	1.125
	$1000_{7.5}$: 250	0.819	1.481	0.553	1.018	0.745	1.366
	1000_{35} : $1000_{7.5}$	1.111	0.892	1.246	0.936	0.723	1.295
Dongwan : Luanchuan		1.265	1.135	1.115	1.034	0.523	1.977
Tantou : Luanchuan		1.185	1.081	1.097	1.048	0.501	2.092

introduced for analyzing slope and channel concentration process. The concentration route distance, the shape and length of stream links, and the slope are determined by DEM resolution and channel threshold.

The relationship among the Manning roughness, the average concentration slope, and the concentration route distance can be established according to the physically based equations (1)–(5). This section was used to study the numerical relationships between different DEM resolutions and catchment scales, so the specific ratio should be considered in the following section: (a) $S_{f_0}^{1/2}$, $S_{f_1}^{1/2}$, L_0, and L_1 in Luanchuan catchment between the resolution of 250 m, 500 m, and 1000 m; (b) $S_{f_0}^{1/2}$, $S_{f_1}^{1/2}$, L_0, and L_1 in Luanchuan catchment between the channel threshold of 7.5 and 35 with the resolution of 1000 m; (c) $S_{f_0}^{1/2}$, $S_{f_1}^{1/2}$, L_0 (unit area), and L_1 (unit area) in nested catchment consisting of Dongwan, Tantou, and Luanchuan. The numerical relationship of n_0 and n_1 with different DEM resolutions, channel thresholds, and catchment scales can be established according to the calculated ratio (Table 3).

2.6. Topographic Index. Topographic Index (TI) [38] refers to the spatial distribution of soil moisture deficiency and runoff process (6). It describes the cumulative trend of runoff in every grid and the slope concentration trend under the effect of gravity [39]. TI of the study catchment can be calculated (Figures 3-4) according to the multiple flow direction algorithm (MFD). As to nested catchment, Dongwan is 11.55, Tantou is 11.44, and Luanchuan is 11.16, which are similar in numerical value and distribution curve (Figure 3). However, they are 11.16, 10.02, and 9.08 for Luanchuan catchment with the DEM resolutions of 1000 m, 500 m, and 250 m, which are quite different in both numerical value and distribution curve (Figure 4).

$$\mathrm{TI} = \ln \frac{\alpha}{\tan \beta}, \tag{6}$$

where α represents the single wide catchment area, and $\tan \beta$ represents the local surface slope.

2.7. Model Parameter Estimation Experiment. Model calibration and validation provide a nominal flow simulation for 13 typical events spanning the period of 1962 to 1998. Selection of events was based on the existence of a flow response at the outlet and obtaining a set of events with a range of peak flow values. In Luanchuan catchment, three resolutions of DEM, which are 250 m, 500 m, and 1,000 m respectively, and

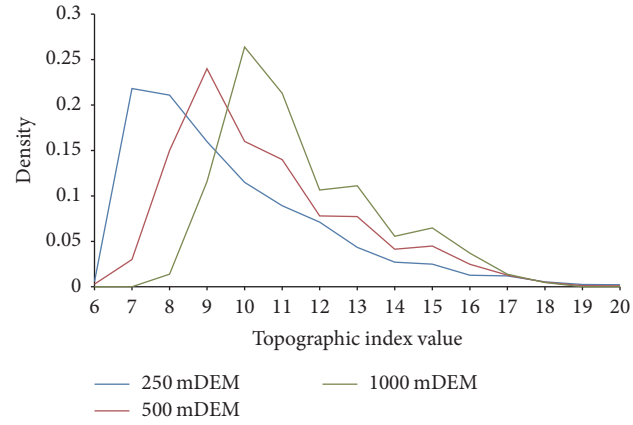

Figure 3: TI of Luanchuan catchment in the DEM resolution of 250 m, 500 m, and 1000 m.

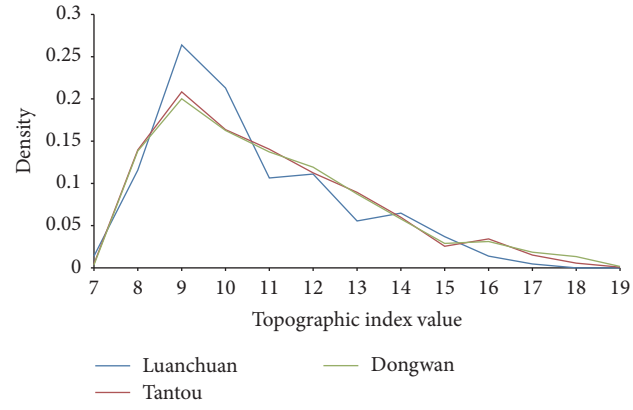

Figure 4: TI of the nested catchment consists of Dongwan, Tantou, and Luanchuan.

two channel thresholds, which are 7.5 and 35 under 1000 m DEM, were adopted to extract the catchment diagram. The parameters of Luanchuan catchment under 250 m DEM resolution could be obtained by parameter calibration based on observed stream flows at catchment-gauged locations through the first 8 flood events. The remaining 5 flood events are validated by the calibrated parameters.

This research regards the nested catchment as highly similar catchments; DEM resolution of 1000 m and channel threshold of 35 are selected to extract catchment diagram. First 8 typical events are selected to calibrate the parameters and 10 events are selected for validation. To compare the

Table 4: Parameters and initial values of Luanchuan catchment.

Resolution	n_0	n_1	Interception	K_s/(cm·h^{-1})	G/cm	M_d
250	0.21	0.05	1.5	0.01	3.5	0.03
500	0.20	0.06				
$1000_{7.5}$	0.12	0.07				
1000_{35}	0.15	0.06				

simulation accuracy in outlet with interior grids, the model parameters were given according to the following two cases: (a) the parameters of Luanchuan should be given first according to Table 4, and the concentration parameters of Tantou and Dongwan catchment should be given according to the numerical relationship shown in Table 3; next, runoff parameters of Tantou and Dongwan are calibrated based on the observed stream flow; (b) Dongwan was considered as a simple catchment, while Tantou and Luanchuan were set as two interior grids. The model parameters of Dongwan were directly calibrated and the simulated flood process of the two interior grids was extracted.

3. Results

3.1. Impact of DEM Resolution and Channel Threshold. According to statistical information of the Luanchuan catchment, the resolution has a significant influence on the grid number and channel threshold has an impact on the length and shape of the drainage line. A smaller channel threshold shows a complex drainage line; on the contrary, a larger channel threshold shows a simple one. The area calculation and spatial distribution of precipitation influenced by DEM resolution can be ignored. The average concentration slope has positive impacts on velocity; the Manning roughness has an adverse effect on velocity, and the route distance is positively related to velocity. In Luanchuan catchment, channel threshold has a significant influence on L_0 (634.82 km to 1289.79 km) and S_{f_0} (0.124 km to 0.153 km); resolution has a major influence on S_{f_0} (0.124 km to 0.185 km) and L_1 (29.64 km to 39.78 km); with the decreasing of DEM resolution, S_{f_0} and L_1 decrease; S_{f_1} is relatively stable when DEM resolution and channel threshold changed. As to the nested catchment, major influence factors are L_0 (1289.79 km to 11010.55 km) and L_1 (27.75 km to 109.31 km). The unit area ratio of L_0 for Dongwan to Luanchuan and Tantou to Luanchuan is near 1.

3.2. Simulation Results. The slope manning roughness n_0 and channel manning roughness n_1 under different resolutions and channel thresholds were given according to the calculated numerical relationship. The precipitation interception coefficient, saturated hydraulic conductivity K_s, saturated head capillary G, and initial soil deficit M_d were calibrated based on observed floods (Table 4). With the decrease of DEM resolution the slope Manning roughness decreases and the channel Manning roughness increases. According to the application in Luanchuan catchment with DEM resolution of 250 m, 500 m, 1000 m, and channel threshold of 35 and 7.5 under the resolution of 1000 m; NSE coefficients are 0.77, 0.76, 0.75, and 0.75; relative errors of peak discharge are −33%, −32%, −36%, and −38% (Figures 5-6). The simulation result with the same runoff parameters and numerical-relationship-based concentration parameters shows the same accuracy. Table 5 provides a summary of the model simulation error, and the simulation error should be represented by a relative error of peak flow and NSE coefficient. Total precipitation of 250 m, 500 m, and 1000 m DEM resolution are 8.50, 8.47, and 8.4 × 10^8 m^3; runoff coefficients are 59.5%, 61.2%, and 63.1%; total runoff is 5.06, 5.18, and 5.32 × 10^8 m^3. The total simulation duration is about 10 d for 250 m DEM, 11 h for 500 m DEM, and only 181 min for 1000 m DEM.

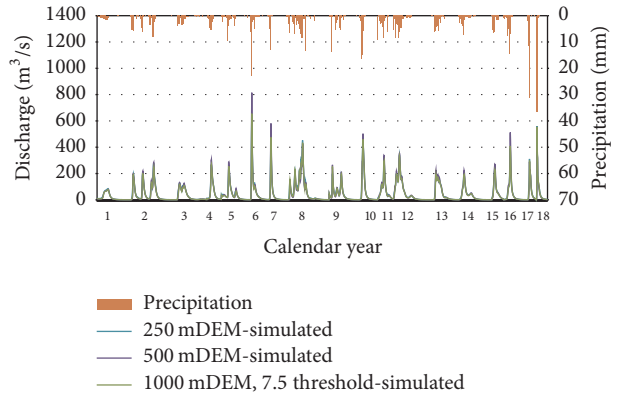

Figure 5: Comparison of the results under the DEM resolution of 250 m, 500 m, and 1000 m.

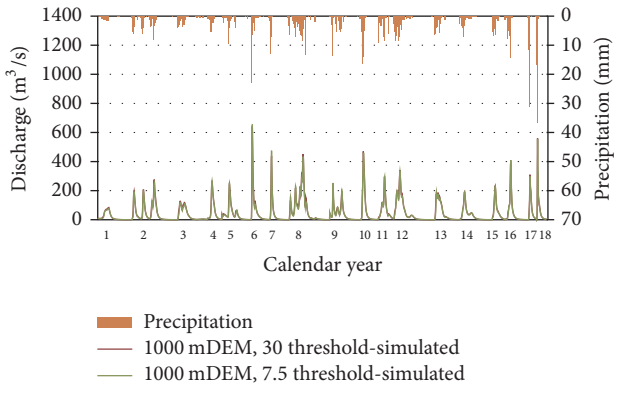

Figure 6: Comparison of the results under the channel thresholds of 7.5 and 35.

3.3. Development of Nested Catchment. For the sensitivity analysis of nested catchment, about 18 typical events were selected for flood simulation and comparison. The simulated runoff parameters and the calculated concentration parameters are shown in Table 6; the simulation and comparison

Table 5: Comparison results under different DEM resolutions and channel thresholds.

Flood time	Relative error of peak discharge				NSE coefficient			
	250 m	500 m	1,000 m_{35}	1,000 $m_{7.5}$	250 m	500 m	1,000 m_{35}	1,000 $m_{7.5}$
1962081406	−12.5	−13.0	−13.1	−14.0	0.48	0.45	0.48	0.46
1963052208	11.0	11.1	10.8	10.5	0.71	0.72	0.75	0.74
1964072300	9.9	11.0	11.2	10.5	0.95	0.92	0.93	0.94
1964100208	5.5	4.9	6.6	6.5	0.85	0.82	0.83	0.83
1965070904	7.5	7.8	8.1	8.2	0.88	0.89	0.84	0.85
1966072200	−10.8	−10.5	−11.8	−12.0	0.72	0.75	0.70	0.70
1967071108	−8.2	−8.5	−9.0	−9.1	0.75	0.76	0.70	0.71
1975080508	10.1	11.2	11.5	11.5	0.80	0.75	0.78	0.77
1975091901	14.3	15.0	14.6	15.5	0.59	0.60	0.59	0.58
1977070900	−17.2	−18.0	−18.8	−19.1	0.47	0.45	0.45	0.46
1980063000	5.6	5.5	5.4	5.8	0.81	0.80	0.76	0.75
1982073102	−8.1	−9.1	−7.9	−7.8	0.89	0.88	0.86	0.85
1983100308	−5.1	−5.2	−5.8	−6.0	0.72	0.73	0.74	0.74
1984090817	−8.5	−8.8	−8.7	−9.0	0.87	0.86	0.85	0.86
1994070220	7.2	6.5	6.6	6.8	0.85	0.83	0.86	0.85
1995081114	3.1	3.8	3.2	3.5	0.88	0.88	0.86	0.85
1996080208	−2.1	−2.0	−2.2	−2.2	0.75	0.75	0.76	0.75
1998081312	−7.7	−7.5	−7.6	−7.8	0.86	0.86	0.83	0.84
Average	−0.33	−0.32	−0.38	−0.46	0.77	0.76	0.75	0.75

Table 6: Parameters and initial values of nested catchment.

Name	n_0	n_1	Interception	K_s/(cm·h^{-1})	G/cm	M_d
Dongwan (simple)	0.16	0.10	1.5	0.01	3.7	0.03
Dongwan	0.17	0.12	1.5	0.01	3.6	0.03
Tantou	0.16	0.13	1.5	0.01	3.8	0.03
Luanchuan	0.15	0.06	1.5	0.01	3.5	0.03

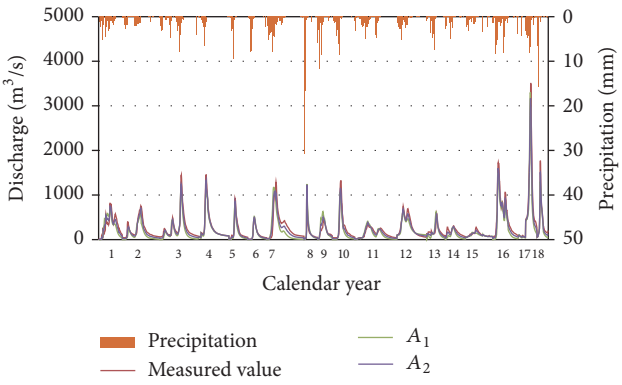

Figure 7: Comparison of the results of Dongwan.

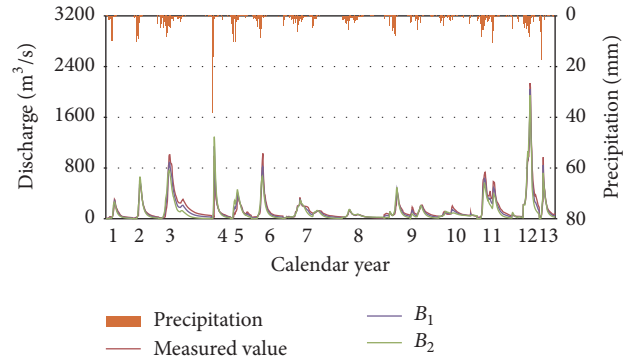

Figure 8: Comparison of the results of Tantou.

results are shown in Figures 7–9. Table 7 lists NSE coefficient and relative error of peak discharge on two different conditions, where A_1, B_1, and C_1 are the simulation results of Dongwan, Tantou, and Luanchuan which are considered as nested catchment; A_2 is the simulation results of Dongwan; B_2 and C_2 are calculated results of Tantou and Luanchuan which are considered as interior grids.

The model performs best in the Luanchuan and worst in the Dongwan in terms of NSE coefficient. Variation of NSE is greatly different in every flood event. The NES of A_1 (from 0.44 to 0.92), B_1 (from 0.52 to 0.91), and C_1 (from 0.45 to 0.93) are much better than A_2 (from 0.42 to 0.90), B_2 (from 0.51 to 0.85), and C_2 (from 0.42 to 0.90). The average NSE coefficient in A_1 (0.70) is the same as A_2 (0.70), and B_1 (0.72) and C_1 (0.75) are larger than B_2 (0.70) and C_2 (0.72). The variation

Table 7: Comparison results of the nested catchment.

Flood time	Relative error of peak discharge (%)						NSE coefficient					
	A_1	A_2	B_1	B_2	C_1	C_2	A_1	A_2	B_1	B_2	C_1	C_2
1962081406	10.0	9.5			−13.1	−11.8	0.81	0.81			0.48	0.42
1963052208	18.5	17.9			10.8	13.2	0.68	0.67			0.75	0.69
1964072300	18.4	16.8			11.2	10.1	0.92	0.90			0.93	0.90
1964092206	29.9	28.5			−3.1	−2.8	0.71	0.72			0.72	0.65
1977070900	−18.1	−17.2	−15.2	−14.8	−18.8	−18.1	0.55	0.55	0.56	0.55	0.45	0.44
1980063000	4.2	4.4	−8.3	−8.5	5.4	5.3	0.77	0.78	0.61	0.60	0.76	0.80
1981071408	−62.5	−62.3	−42.5	−42.4	3.1	3.0	0.65	0.63	0.80	0.79	0.88	0.85
1982073102	33.2	33.5	13.0	14.2	−7.9	−9.2	0.70	0.71	0.82	0.80	0.86	0.80
1983081020	5.2	4.2	3.3	3.4			0.81	0.82	0.72	0.72		
1983100308	−6.2	−6.3	2.2	2.3	−5.8	−5.2	0.44	0.42	0.61	0.55	0.74	0.69
1983101708	20.5	20.0	12.8	12.5			0.64	0.63	0.58	0.55		
1984090817	6.8	6.3			−8.7	−8.2	0.83	0.80			0.85	0.81
1985091412	−6.2	−6.0	−12.8	−12.8			0.72	0.73	0.74	0.73		
1988080909	−30.5	−30.2	−22.5	−22.4			0.48	0.49	0.52	0.51		
1989081408	−22.5	−22.0	−13.6	−13.5			0.62	0.63	0.81	0.82		
1996080208	19.5	19.3	8.5	8.2	−2.2	−11.2	0.78	0.76	0.91	0.85	0.76	0.73
1998081312	−10.2	−11.0	2.5	2.8	−7.6	−8.3	0.81	0.80	0.80	0.77	0.83	0.85
2000071220	33.3	33.0	1.2	1.5	−40.5	−41.4	0.66	0.67	0.82	0.81	0.75	0.75
Average	2.41	2.13	−5.49	−5.35	−5.94	−6.5	0.70	0.70	0.72	0.70	0.75	0.72

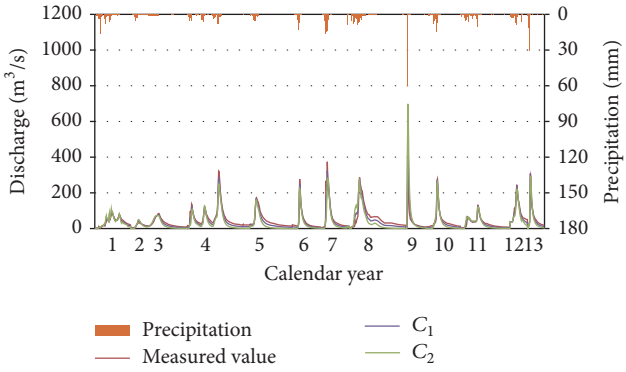

Figure 9: Comparison of the results of Luanchuan.

of relative error of peak discharge in B_1 (from −42.5% to 13.0%) and C_1 (from −40.5% to 11.2%) is smaller than B_2 (from −42.4% to 14.2%) and C_2 (from −41.4% to 13.2%).

4. Discussion

CASC2D model is a catchment-based hydrological model with distributed inputs and distributed parameters, which was used for accurate hydrological information simulation in small scale catchment with high DEM resolution [27, 32]. This study investigated the influence factors and sensitive parameters to improve the accuracy and efficiency of physically based distributed hydrological model. Parameter analysis shows that K_s, G, and M_d varied slightly in different resolutions, channel thresholds, and catchment scales when they were used as runoff parameters. L_0, L_1, S_{f_0}, and S_{f_1} played a dominant role in controlling the n_0 and n_1.

Input information (i.e., precipitation, soil, vegetation, and other underlying surface conditions) which is influenced by DEM resolution and channel threshold plays an important role in controlling the simulation process. The inverse square distance weighting is an excellent method to interpolate the rainfall in spatial scales [40, 41]. However, it is still difficult to describe the uneven distribution of rainfall in temporal scales, which makes the Green-Ampt equation and its parameters inefficient when an hourly interval rainfall data is used. There is a precipitation station for every 170 km^2 in Luanchuan, 307 km^2 in Tantou, and 321 km^2 in Dongwan, which makes the NES coefficient and relative error of peak discharge the best in Luanchuan and the worst in Dongwan. It highlights the significance of raw data and interpolation methods both in spatial and in time scales.

Lower DEM resolution would limit the attributes of each grid [42] and further restrict the simulation of hydrological attributes in interior grids. TI was greatly influenced by the resolution and information content of a DEM [43], and it was regarded as an important index to describe the rainfall-runoff process. Calculated TI shows a great difference in Luanchuan and the same in the nested catchment, which means the similarity should be established based on the same DEM resolution. On the one hand, with 1,000 m DEM resolution in Tantou and Luanchuan, the simulation results are superior to the calculated interior grids when parameters are reasonably calibrated. These simulation results indicate the uncertainty of interior grids in distributed hydrological model. The input information, parameters, and physical equations need to be more reasonable with the change of scale and position. On the other hand, Dongwan always served as an outlet, no matter when simulated in the nested catchment or as a simple catchment. The calibrated parameters are different and the

simulation results are revealed to be the same, which reveals a phenomenon of equifinality for different parameters.

According to the statistical hydrological information, the concentration parameters could be given reasonably, which could offset the error caused by DEM processing and improve the simulation accuracy in interior grids. Sensitivity analysis and scale change regulation of parameters are necessary and helpful for parameter transplantation and accuracy improvement with parameters reasonably given.

The physically based model links the laboratory scales and field application scales, which provides a basis to calibrate parameters. However, it is still difficult to use the measured parameters in hydrological model. So parameter calibration and validation are necessary and urgently needed. The statistics of influence factors and sensitive parameters provide the variations of runoff process as well as concentration parameters. In order to establish a more accurate relationship in different scales, more data regarding rainfall, discharge, groundwater distribution, accurate DEM, soil structure, and vegetation are needed.

5. Conclusions

The study was conducted to find the sensitive influence factors and parameters of the physically based distributed hydrological model. Three kinds of DEM resolutions and two kinds of channel thresholds are used in Luanchuan to analyze the variation of the catchment area, precipitation, slope, and concentration route distance. It reflects a clear and regular variation of L_0, L_1, S_{f_0}, and S_{f_1}, which can build a relationship with n_0, and n_1.

Considering NSE coefficient and relative error of peak discharge of the simulation results, the results show the same accuracy when runoff parameters are not changed and concentration parameters are reasonably given by the established relationship. Hence, the study suggests that the appropriate DEM resolutions and channel thresholds should be used in different needs. Considering the computational efficiency, low-precision DEM data are more suitable when the parameters can be reasonably given.

According to the statistic and calculated information about the nested catchment, the contrasting results need to be doubted for accuracy and rationality in calculated grids. It is observed that the more accurate simulation results are simulated in Tantou and Luanchuan when calibrated parameters are used, which confirms the reasonability of the established relationship. However, further improvement of simulation accuracy requires a more accurate description of precipitation and more precise underlying surface data in spatial and temporal scales.

Competing Interests

The authors declare no conflict of interests.

Acknowledgments

This work was supported by the National Natural Science Foundation of China (Grant nos. 41130639, 51179045, and 41201028) and the Non-Profit Industry Financial Program of MWR of China (nos. 201501022 and 201301068).

References

[1] M. B. Smith, D.-J. Seo, V. I. Koren et al., "The distributed model intercomparison project (DMIP): motivation and experiment design," *Journal of Hydrology*, vol. 298, no. 1–4, pp. 4–26, 2004.

[2] K. Beven, "Changing ideas in hydrology—the case of physically-based models," *Journal of Hydrology*, vol. 105, no. 1-2, pp. 157–172, 1989.

[3] V. Y. Ivanov, E. R. Vivoni, R. L. Bras, and D. Entekhabi, "Preserving high-resolution surface and rainfall data in operational-scale basin hydrology: a fully-distributed physically-based approach," *Journal of Hydrology*, vol. 298, no. 1–4, pp. 80–111, 2004.

[4] M. Sivapalan, K. Beven, and E. F. Wood, "On hydrologic similarity: 2. A scaled model of storm runoff production," *Water Resources Research*, vol. 23, pp. 2266–2278, 1987.

[5] L. Liuzzo, L. V. Noto, E. R. Vivoni, and G. La Loggia, "Basin-scale water resources assessment in Oklahoma under synthetic climate change scenarios using a fully distributed hydrologic model," *Journal of Hydrologic Engineering*, vol. 15, no. 2, pp. 107–122, 2010.

[6] M. Sivapalan, K. Takeuchi, S. W. Franks et al., "IAHS Decade on Predictions in Ungauged Basins (PUB), 2003–2012: shaping an exciting future for the hydrological sciences," *Hydrological Sciences Journal*, vol. 48, no. 6, pp. 857–880, 2003.

[7] K. Beven and A. Binley, "The future of distributed models: model calibration and uncertainty prediction," *Hydrological Processes*, vol. 6, no. 3, pp. 279–298, 1992.

[8] P. Yang, D. P. Ames, A. Fonseca et al., "What is the effect of LiDAR-derived DEM resolution on large-scale watershed model results?" *Environmental Modelling & Software*, vol. 58, pp. 48–57, 2014.

[9] M. Bierkens, P. Finke, and P. De Willigen, *Upscaling and Downscaling Methods for Environmental Research*, Springer, 2000.

[10] M. Sivapalan, R. Grayson, and R. Woods, "Scale and scaling in hydrology," *Hydrological Processes*, vol. 18, pp. 1369–1371, 2004.

[11] R. Rojas, P. Julien, and B. Johnson, "A 2-dimensional rainfall-runoff and sediment model," CASC2D-SED. Reference Manual, Colorado State University, Fort Collins, Colo, USA, 2003.

[12] K. J. Beven, *Rainfall-Runoff Modelling: The Primer*, John Wiley & Sons, New York, NY, USA, 2011.

[13] K. Beven, "Linking parameters across scales: subgrid parameterizations and scale dependent hydrological models," *Hydrological Processes*, vol. 9, no. 5-6, pp. 507–525, 1995.

[14] G. Blöschl, "Scaling in hydrology," *Hydrological Processes*, vol. 15, pp. 709–711, 2001.

[15] V. P. Singh, "Watershed modeling," in *Computer Models of Watershed Hydrology*, pp. 1–22, 1995.

[16] J. Zhang and X. Chu, "Impact of DEM resolution on puddle characterization: comparison of different surfaces and methods," *Water*, vol. 7, no. 5, pp. 2293–2313, 2015.

[17] R. H. Erskine, T. R. Green, J. A. Ramirez, and L. H. MacDonald, "Comparison of grid-based algorithms for computing upslope contributing area," *Water Resources Research*, vol. 42, no. 9, Article ID W09416, 2006.

[18] J. Yang and X. Chu, "Effects of dem resolution on surface depression properties and hydrologic connectivity," *Journal of Hydrologic Engineering*, vol. 18, no. 9, pp. 1157–1169, 2013.

[19] M. W. Gitau and I. Chaubey, "Regionalization of swat model parameters for use in ungauged watersheds," *Water*, vol. 2, pp. 849–871, 2010.

[20] H. Wan, J. Xia, L. Zhang, D. She, Y. Xiao, and L. Zou, "Sensitivity and interaction analysis based on Sobol' method and its application in a distributed flood forecasting model," *Water*, vol. 7, no. 6, pp. 2924–2951, 2015.

[21] Y. Gan, Q. Duan, W. Gong et al., "A comprehensive evaluation of various sensitivity analysis methods: a case study with a hydrological model," *Environmental Modelling & Software*, vol. 51, pp. 269–285, 2014.

[22] C.-S. Zhan, X.-M. Song, J. Xia, and C. Tong, "An efficient integrated approach for global sensitivity analysis of hydrological model parameters," *Environmental Modelling & Software*, vol. 41, pp. 39–52, 2013.

[23] A. Van Griensven, T. Meixner, S. Grunwald, T. Bishop, M. Diluzio, and R. Srinivasan, "A global sensitivity analysis tool for the parameters of multi-variable catchment models," *Journal of Hydrology*, vol. 324, no. 1–4, pp. 10–23, 2006.

[24] O. Rakovec, M. C. Hill, M. P. Clark, A. H. Weerts, A. J. Teuling, and R. Uijlenhoet, "Distributed evaluation of local sensitivity analysis (DELSA), with application to hydrologic models," *Water Resources Research*, vol. 50, no. 1, pp. 409–426, 2014.

[25] P. Julien and R. Rojas, "Upland erosion modeling with casc2d-sed," *International Journal of Sediment Research*, no. 4, pp. 265–274, 2002.

[26] M. Marsik and P. Waylen, "An application of the distributed hydrologic model CASC2D to a tropical montane watershed," *Journal of Hydrology*, vol. 330, no. 3-4, pp. 481–495, 2006.

[27] S. U. S. Senarath, F. L. Ogden, C. W. Downer, and H. O. Sharif, "On the calibration and verification of two-dimensional, distributed, hortonian, continuous watershed models," *Water Resources Research*, vol. 36, no. 6, pp. 1495–1510, 2000.

[28] W. H. Green and G. Ampt, "Studies on soil phyics," *The Journal of Agricultural Science*, vol. 4, pp. 1–24, 1911.

[29] M. New, M. Hulme, and P. Jones, "Representing twentieth-century space-time climate variability. Part I: development of a 1961-90 mean monthly terrestrial climatology," *Journal of Climate*, vol. 12, no. 2-3, pp. 829–856, 1999.

[30] W. J. Rawls, D. L. Brakensiek, and N. Miller, "Green-ampt infiltration parameters from soils data," *Journal of Hydraulic Engineering*, vol. 109, no. 1, pp. 62–70, 1983.

[31] F. L. Ogden, "De st-venant channel routing in distributed watershed modeling," in *Proceedings of the ASCE Hydraulics Division Specialty Conference*, pp. 492–496, Buffalo, NY, USA, August 1994.

[32] C. W. Downer, F. L. Ogden, W. D. Martin, and R. S. Harmon, "Theory, development, and applicability of the surface water hydrologic model CASC2D," *Hydrological Processes*, vol. 16, no. 2, pp. 255–275, 2002.

[33] P. Y. Julien, B. Saghafian, and F. L. Ogden, "Raster-based hydrologic modeling of spatially-varied surface runoff," *Journal of the American Water Resources Association*, vol. 31, no. 3, pp. 523–536, 1995.

[34] S. Kienzle, "The effect of DEM raster resolution on first order, second order and compound terrain derivatives," *Transactions in GIS*, vol. 8, no. 1, pp. 83–111, 2004.

[35] W. Z. Shi and Y. Tian, "A hybrid interpolation method for the refinement of a regular grid digital elevation model," *International Journal of Geographical Information Science*, vol. 20, no. 1, pp. 53–67, 2006.

[36] J. Vaze, J. Teng, and G. Spencer, "Impact of DEM accuracy and resolution on topographic indices," *Environmental Modelling & Software*, vol. 25, no. 10, pp. 1086–1098, 2010.

[37] R. H. Erskine, T. R. Green, J. A. Ramirez, and L. H. MacDonald, "Digital elevation accuracy and grid cell size: effects on estimated terrain attributes," *Soil Science Society of America Journal*, vol. 71, no. 4, pp. 1371–1380, 2007.

[38] Z. Qiu, "Validation of a locally revised topographic index in Central New Jersey, USA," *Water*, vol. 7, no. 11, pp. 6616–6633, 2015.

[39] P. F. Quinn, K. J. Beven, and R. Lamb, "The in(a/tanβ) index: how to calculate it and how to use it within the Topmodel framework," *Hydrological Processes*, vol. 9, no. 2, pp. 161–182, 1995.

[40] F.-W. Chen and C.-W. Liu, "Estimation of the spatial rainfall distribution using inverse distance weighting (IDW) in the middle of Taiwan," *Paddy & Water Environment*, vol. 10, no. 3, pp. 209–222, 2012.

[41] S. Janapriya and S. S. Bosu, "Assessment of spatial variability of rainfall data using inverse distance weighting (idw) in the manjalar sub-basin of vaigai in tamil nadu," *Trends in Biosciences*, vol. 7, no. 21, pp. 3396–3401, 2014.

[42] I. Chaubey, A. S. Cotter, T. A. Costello, and T. S. Soerens, "Effect of DEM data resolution on SWAT output uncertainty," *Hydrological Processes*, vol. 19, no. 3, pp. 621–628, 2005.

[43] R. Sørensen and J. Seibert, "Effects of DEM resolution on the calculation of topographical indices: TWI and its components," *Journal of Hydrology*, vol. 347, no. 1-2, pp. 79–89, 2007.